Indian Journal of Chemistry
Vol. 59A, May 2020, pp. 608-615

Synthesis, spectral studies and antibacterial activity of iron(III) complexes with hydrazone functionalized ligands: X-Ray structure determination of a novel five coordinate complex containing labile ligands

Dudekula Kasimbi[a], Katreddi Hussain Reddy[a]* & N. Devanna[b]

[a]Department of Chemistry, Sri Krishnadevaraya University, Ananthapuramu 515 003, India
[b]Department of Chemistry, Jawaharlal Nehru Technological University, Anaanthapuramu 515 001, India
Email: khussainreddy@yahoo.co.in

Received 17 January 2020; revised and accepted 27 April 2020

Iron(III) complexes having general formula $FeLCl_2$ [where, L = 2-acetylpyridine acetoylhydrazone (APAH), 2-acetylpyridine benzoylhydrazone (APBH), 2-acetylthiophene acetoylhydrazone (ATAH), and 2-acetythiophene benzoylhydrazone (ATBH)] have been synthesized and characterized based on molar conductivity, electronic and IR spectroscopy. The structure of iron(III) complex with APBH ligand is determined using single crystal X-ray crystallography. The complex crystallizes in monoclinic space group P21/n with a = 7.8490(6) Å, b = 15.1018(11) Å, c = 13.2263(10) Å, α = 90°, β=100.183(3)°, γ = 90°, V = 1543.1(2) $Å^3$ and Z = 4 with central Fe(III) ion coordinated by one tridentate APBH ligand. The iron is involved in 5-coordinate bonding with one organic (hydrazone) unit and two labile chloride ligands. The ligand acts as NNO–tridentate donor system. Iron is coordinated to pyridine ring nitrogen, azomethine nitrogen and benzoyl oxygen atoms and the two chloride ligands bind with metal completing distorted square pyramidal structure. The ligands and iron complexes are screened for their anti-bacterial activities against *Pseudomonas aureoginos* and *Bacillus cereus*. Among ligands, acetoyl hydrazones show more activity than the corresponding benzoyl hydrazones. The hydrazones having a methyl/ and pyridine groups show higher antibacterial activity. The iron complexes show higher activity than the metal free ligands.

Keywords: Iron(III) complexes, Trifunctional donor ligands, Crystal structure, Antibacterial activity.

A good number of penta-coordinated prosthetic groups play vital roles in biological processes[1]. For example, in respiration, iron is 5-coordinate in deoxy state of iron proteins such as myoglobin and hemoglobin. Further, zinc is pentacoordinate in carbonic anhydrase, in working state of enzyme. Interestingly, copper is 5-coordinate in superoxide dismutase (SOD). Hence it is of interest to investigate[2] pentacoordinated metal complexes.

Organic ligands, particularly, hydrazones constitute important class of medicinal compounds due to their wide variety of pharmacological and analytical applications[3-5]. They also bestow applications in floral arena as plant growth regulators[6, 7]. Hydrazones are versatile class of ligands having a wide range of biological activities such as antimicrobial[8], anti-tubercular[9], anticonvulsant[10], anti-inflammatory[11], cytotoxic[12] and vasodilator[13] activities. Hydrazones derived from pyridine carbonyls are known to inhibit the proliferation of tumor cells to a greater extent compared to standard anticancer agents[14, 15].

Hydrazones, particularly tridentate functionalized ligands have recently attracted considerable interest[16-20]. Inorganic chemists have been motivated by a wide variety of biological and pharmaceutical activities[21-26] of hydrazones. The tautomerism of these ligands allows various structural possibilities[27] for the corresponding metal complexes. In addition, the versatile applications of metal complexes with hydrazone functionalized ligand in the field of biological[28-30] and industrial processes[31,32] prompted us to synthesize hydrazone functionalized pyridine/thiophene ligands and their iron(III) complexes. Jang *et al*[33] have reported synthesis and spectral characterization of Mn(II), Co(II), Ni(II), Cu(II), and Zn(II) complexes with 2-acetylpyridinebenzoylhydrazone (APBH) and structures of Mn(II) and Zn(II) complexes with ATBH are determined. However, there is no report on the structure determination of Fe(III) complex with APBH ligand.

In the light the above and biological importance of pentacoordinate metal complexes in biological processes and in continuation of our ongoing research work[34-38], herein we report synthesis, spectral characterization, antibacterial activity and single

crystal X-ray structure determination of novel five coordinate iron(III) complex of APBH.

Materials and Method

All the chemicals and ferric chloride used were of AR grade. Ferric chloride, 2-acetylpyridine, 2-acetylthiophene, acetic hydrazide and benzhydrazide were purchased from Sigma-Aldrich India chemical company and were used without further purification.

Synthesis of 2- Acetylpyridine acetoylhydrazone (APAH)

A 2.96 g (0.04 mol) of acetic hydrazide dissolved in 20 ml methanol was added to a hot methanolic solution (20 ml) of 2-acetylpyridine (0.04 mol, 5 ml) in a 100 ml round bottom flask. Glacial acetic acid (3-4 drops) was added to the reaction mixture and refluxed over water bath for 2 h and cooled to room temperature. The crystalline compound formed was collected by filtration, washed several time with hot water and dried in vacuo. It was recrystallised from methanol. Yield: 85%; M.P:162–164 ^{o}C; ; Analytical data %C, 61.49(61.01); %H, 6.21(6.25); %N, 23.65(23.71); IR spectra (KBr, cm^{-1}) 3185(br) (υ_{NH}); 1678(s) ($\upsilon_{C=O}$); 1620(s) ($\upsilon_{C=N}$); ^{1}H NMR ($CDCl_3$,300 MHz): δ 2.28(s, 3H,-CH_3 acetoyl); 2.35(s, 3H,-CH_3 acetyl); 7.25(s, 1H, NH); 7.75-7.85 (m, 4H, Pyridine); ^{13}C NMR (125 MHz $CDCl_3$): δ 173.6, 155.1, 148.6, 148.2, 136.2. 123.7, 12 0.2, 20.6 and 10.7; GC-MS, m/z, 177 (M^+).

Synthesis of 2- Acetyylpyridine benzoylhydrazone (APBH)

A solution of benzhydrazide (5.44 g, 0.04 mol) in 20 ml methanol was added to hot methanolic solution (20 ml) of 2-acetyl pyridine (0.04 mol, 5 ml) in a 100 ml round bottom flask. Few drops of glacial acetic acid were added to the reaction mixture. The pale white powdered compound formed was filtered off, washed several times with hot water and dried in vacuo. It was recrystallized from methanol. Yield: 80% M.P.: 145–147 ^{o}C; Analytical data %C, 69.60(70.27); %H, 5.63(5.47); %N, 17.72(17.56); IR spectra (KBr, cm^{-1}) 3177(br)(υ_{NH}); 1651(s) ($\upsilon_{C=O}$); 1616(s) ($\upsilon_{C=N}$); ^{1}H NMR ($CDCl_3$, 300 MHz): δ 2.51(s, 3H,-CH_3 Acetyl H); 7.25 (s, 1H, NH); 7.75-7.85 (m, 9H, Phenyl and Pyridine H); ^{13}C NMR (125 MHz $CDCl_3$): δ 163.9, 154.9, 153.0, 148.5, 136.3, 133.4, 132.1, 130.3, 128.7, 127.4, 124.0, 121.4, 120.5, and 11.2. GC-MS, m/z, 239 (M^+).

Synthesis of 2- Acetylthiophene acetoylhydrazone (ATAH)

A 2.96 g (0.03 mol) of acetic hydrazide dissolved in 20 ml methanol was added to a hot methanolic solution (20 ml) of 2-acetylthiophene (0.03 mol, 5.03 ml) in a 100 ml round bottom flask. Glacial acetic acid (3-4 drops) was added to the reaction mixture. The contents were refluxed over water bath for 2 h and cooled to room temperature. The crystalline compound formed was collected by filtration, washed several times with hot water and dried in vacuo. It was recrystallized from methanol. Yield: 85% M.P.:176-178 ^{o}C; Analytical data %C, 53.25(52.74); %H, 5.52(5.49); %N, 15.30(15.38); IR spectra (KBr, cm^{-1}) 3174(br)(υ_{NH}); 1666(s)($\upsilon_{C=O}$); 1606(s) ($\upsilon_{C=N}$); ^{1}H NMR ($CDCl_3$, 300 MHz): δ 2.35(s, 3H, -CH_3 acetoyl); 2.45(s, 3H, -CH_3 acetyl); 9.50(s, 1H, NH); 7.00-7.30 (m, 3H, thiophene); ^{13}C NMR (125 MHz $CDCl_3$): δ 174.8, 143..8, 127.6, 127.3, 126.4, 20.5 and 13.5; GC-MS, m/z, 212 (M^+).

Synthesis of 2- Acetylthiophene benzoylhydrazone (ATBH)

A 3 g (0.02 mol) of benzhydrazide dissolved in 20 ml methanol was added to a hot methanolic solution (20 ml) of 2-acetyl thiophene (0.03 mol, 2.7 ml) in a 100 ml round bottom flask. Glacial acetic acid (3-4 drops) was added to the reaction mixture. The contents were refluxed over water bath for 2 h and cooled to room temperature. The crystalline compound formed was collected by filtration, washed several times with hot water and dried in vacuo. It was recrystalized from methanol. Yield, 85%, M.P. 198-200 ^{o}C. Analytical data %C, 64.50(63.93); %H, 4.85(4.91); %N, 11.60(11.47); IR spectra (KBr, cm^{-1}) 3327(br)(υ_{NH}); 1651(s)($\upsilon_{C=O}$); 1608(s) ($\upsilon_{C=N}$); ^{1}H NMR ($CDCl_3$,300MHz): δ 2.51(s, 3H, -CH_3 acetyl); 7.25(s, 1H, NH); 7.75-7.85 (m, 3H, thiophene); ^{13}NMR (125 MHz $CDCl_3$): A good spectrum is not obtained as the sample has low solubility; GC-MS, m/z, 248 (M^+).

Synthesis of Iron(III) complexes

To an ethanolic solution of hydrazone (0.02 mol) taken in a 100 ml round bottom flask, an aqueous solution of $FeCl_3$ (0.162 g, 0.01 mol) was added and the reaction mixture was heated on a water bath under reflux for 3 h. The reaction mixture was cooled to room temperature. A colored product separated out was collected by filtration, washed with ethanol followed by hexane and dried in vacuum. **Fe(APAH)Cl_2:** M. W. 304; Colour, Dark Brown; Yield, 92% ; M.P.:203–208 ^{o}C; Analytical data, %C, 35.20(35.55); %H, 3.31(3.29); %N, 13.75(13.82) Fe, 18.20(18.28); IR spectra (KBr, cm^{-1}), 1605(s) ($\upsilon_{C=N}$); 510(m) (υ_{Fe-N}); 450(m) (υ_{Fe-O}); 340(w) (υ_{Fe-Cl}); Molar conductivity (Ω^{-1} cm^2 mol^{-1}), 6. **Fe(APBH)Cl_2:** M. W. 365; Colour, Black;

Yield, 80%; M.P.265–268 ^{o}C; Analytical data, %C, 45.70(46.03); %H, 3.25(3.28); %N, 11.65(11.50) Fe, 15.40(15.30); IR spectra (KBr, cm^{-1}), 1589(s)($\upsilon_{C=N}$); 508(m) (υ_{Fe-N}); 445(m) (υ_{Fe-O}); 335(w)(υ_{Fe-Cl}); Molar conductivity (Ω^{-1} cm^2 mol^{-1}), 10. **Fe(ATAH)Cl_2:** M. W. 308; Colour, Brown ; Yield, 60% ; MP. 209-212 ^{o}C ; Analytical data, %C, 30.75(31.16); %H, 2.85(2.92); %N, 8.90(9.00) Fe, 17.70(18.13); IR spectra (KBr, cm^{-1}), 1580(s) ($\upsilon_{C=N}$); 500(m) (υ_{Fe-N}); 440(m) (υ_{Fe-O}); 353(w) (υ_{Fe-Cl}); Molar conductivity (Ω^{-1} cm^2 mol^{-1}), 9. **Fe(ATBH)Cl_2:** M. W. 370; Colour, Brow ; Yield, 75% ; MP. 262-263 ^{o}C; Analytical data, %C, 41.90(42.16); %H, 2.85(2.97); %N, 7.70(7.56) Fe, 14.90(15.10);); IR spectra (KBr, cm^{-1}), 1602(s) ($\upsilon_{C=N}$); 590(m) (υ_{Fe-N}); 442(m) (υ_{Fe-O}); 353(w) (υ_{Fe-Cl}); Molar conductivity (Ω^{-1} cm^2 mol^{-1}), 10.

Instrumentation

The melting points were determined using Buchi B450 melting point apparatus. Molar conductivity was measured in dimethyl formamide (DMF) (10^{-3} M) at 25 ^{o}C on an ELICO CM 180 digital conductivity bridge. Mass spectra of the ligands were recorded on JEOL GC MATE II GC-Mass spectrometer in EI^{+} ionization mode. Elemental analyses were performed using Perkin Elmer 2400 CHN analyzer. ^{1}H NMR spectra were recorded at room temperature on a Brucker Avance II 400 FT-NMR spectrometer using DMSO d_6 as solvent and tetra methyl silane (TMS) as internal reference. The electronic spectra were recorded in DMF with a Perkin Elmer UV Lamda -50 spectrophotometer. FTIR spectra in KBr disc were recorded in the range 4000-400 cm^{-1} with a Perkin Elmer spectrum 100 spectrometer. The ESI (+) mass spectra were recorded on a water ZQ-4000 liquid chromatography- mass spectrometer. The ^{1}H (300 MHZ) NMR spectra were recorded at room temperature on a Bruker Avance II 400 FT-NMR spectrometer at 27 ^{o}C, using DMSO-d_6 as solvent and tetramethylsilane (TMS) as internal standard.

Crystal data were collected by using the Enraf Nonius CAD4-MV31 single crystal X-ray diffractometer, Indian Institute of Technology Madras, Chennai. Enraf Nonius CAD_4-$MV_3$1 single crystal X-ray diffractometer is a fully automated four circle instrument controlled by a computer. It consists of an FR 590 generator, a goniometer, CAD_4F interface and a micro$VAX_3$100 equipped with a printer and plotter. The detector is a scintillation counter. A single crystal is mounted on a thin glass fiber fixed on the goniometer head. The unit cell dimensions and orientation matrix are determined using 25 reflections and then the intensity data of a given set of reflections are collected automatically by the computer. An IBM compatible PC/AT 486 is attached to micro VAX facilitating the data transfer on to a DOS floppy of 5.25" or 3.5". Maximum X-ray power is 40 mA x 50 KV. The data collected were reduced using SAINT program[39] The trial structure was obtained by direct method[40] using SHELXS-86, which revealed the position of all non-hydrogen atoms and refined by full-matrix least squares on F^2 (SHELXS-97)[41] and graphic tool was DIAMOND for windows[42]. All non-hydrogen atoms were refined anisotropically, while the hydrogen atoms were treated with a mixture of independent and constrained refinements.

Antibacterial activity:

Sample solutions were prepared with different amounts (200, 300 and 500 µg) of each compound in DMF that had no influence on the microbial growth. *Bacillus cereus* (MTCC 1305) and *Pseudomonas aureoginosa* (MTCC 2453) were chosen based on their clinical and pharmacological importance. The bacterial strains were obtained from Department of Microbiology, Osmania University, Hyderabad. The bacterial stock cultures were incubated for 24 h at 37 °C on nutrient agar. The bacteria were grown on Mueller-Hinton agar plates at 37 °C. Antibacterial activities of ligands and iron(III) complexes were determined by zone inhibition method.

Preparation of discs:

Whatman No.1 filter paper discs of 5 mm diameter were autoclaved by keeping in a clean and dry Petri plate. The discs were soaked in compound solutions for 5 h were taken as test material. After 5 h the discs were shade dried. The concentrations of compound solutions per disc are accounted for 0.1 g/ml. Subsequently they were carefully transferred to spread on cultured Petri plates. Filter paper discs immersed in ethanol are prepared and used as positive control and streptomycin as negative control.

Testing of antibacterial activity:

Lysogeny broth (LB) agar medium was prepared and the medium was sterilized at 121 °C for 30 min. The agar plates were prepared by pouring about 10 ml of the medium into 10 cm Petri dishes under aseptic condition and left undisturbed for 2 h to solidify the medium. A 1 ml aliquot of inoculum of bacteria (1-5 x 10^8 CFU/ml) was poured on to the plates separately containing solidified agar media. The

prepared sterile filter paper discs were impregnated with the compound solutions and shaken thoroughly and these test plates incubated for a period of 48 h at 37 ºC for the development of inhibitory zones and the average of two independent readings for each organism in different compound solutions were recorded. The inhibition zones were measured after 1 day at 37 ºC for bacteria. The diameter of the inhibition zone was measured and recorded with the aid of plastic ruler. Five paper discs placed in one Petri plate.

Results and Discussion

The ligands viz. 2-acetylpyridine acetoylhydrazone (APAH), 2-acetylpyridine benzoylhydrazone (APBH), 2-acetylthiophene acetoylhydrazone (ATAH), and 2-acetylpyridine benzoylhydrazone (ATBH) are synthesized and characterized based on IR, ^{1}H NMR and mass spectral data. Structures of the ligands are shown in Fig. 1. The iron(III) complexes of these ligands are obtained in good yields. The complexes are stable at room temperature and non-hygroscopic. The complexes are partially soluble in water, less soluble methanol and ethanol and readily soluble in acetonitrile (CH_3CN), DMF and DMSO. The molar conductivity values (6-10 Ω^{-1} cm^2 mol^{-1}) suggest that the complexes are non-electrolytes[43].

Spectral characterization

The absorption spectra of complexes exhibit two intense absorption bands in the ranges 265–280 and 350–375 nm, which are assigned to pyridine nitrogen ($p\pi$) → Fe(III) ($d\sigma^*$) and pyridine nitrogen ($p\pi$) → Fe(III) ($d\pi^*$) LMCT transitions[44], respectively (Fig. S1, Supporting Data). Bands due to d-d transitions are not observed as strong charge transfer (CT) band tailing from the UV region to the visible region[45]. FTIR spectra of complexes in the region 4000–400 cm^{-1} are analyzed in comparison with that of the spectra of metal free hydrazone ligands (Figs, S2–S5). IR spectra of complexes are similar in relative positions and intensities of the peaks, which suggest a close structural relationship among compounds. The IR spectra of free ligands show strong peaks in the 1651–1678 cm^{-1} region, which are attributable to stretching vibration of the amido carbonyl ($\nu_{>C=O}$ group). This band disappears in the spectra of all iron complexes due to enolization of >C=O group and formation of covalent bond between oxygen and iron(III). The vibrational bands in IR spectra of ligands in the 1606-1620 cm^{-1} region are assigned to the ν (C=N) of the azomethine. These bands are shifted to lower wave numbers on complexation indicating the participation of azomethine nitrogen in coordination to the iron[4]. The vibrational bands in the 3174 –3327 cm^{-1} region can be assigned to the ν(N-H) for the free ligand. The ν(N-H) bands disappeared in the spectra of iron complexes due to the enolization and concomitant covalent bond formation between oxygen and iron(III). These observations suggest that the present hydrazones act as monoanionic tridentate ligands. The pyridine and thiophene ring deformation modes observed in 620–625 and 710–715 cm^{-1} regions, respectively in the spectra of ligands. These bands shifted to higher wave number indicating coordination of hetrocyclic nitrogen and sulphur to iron atom. The new bands in 500–510, 440–450 and 335–359 cm^{-1} regions are assigned to ν(Fe–N) and ν(Fe–O) and ν(Fe–Cl) vibration, respectively. The tridentate behavior of ligands and the composition of complexes are in analogy with our previous observation[47].

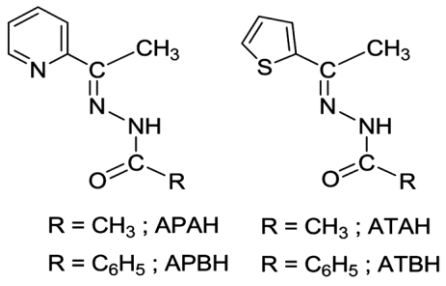

Fig. 1 — Structures of functionalized ligands.

Description of molecular structure of Fe(APBH)Cl$_2$

Crystal data and structure refinement parameters are given in Table 1. Selected bond lengths and bond angles are given in Table 2. ORTEP view of Fe(APBH)Cl$_2$ together with atom labelling scheme is used as shown in Fig. 2. The compound Fe(APBH)Cl$_2$ crystallize in monoclinic, space group $P2_1/n$ and the structure contains six monomeric neutral complex molecules in each unit cell, as shown in Fig. 3. Iron atom is surrounded by five coordinated donor atoms. Three of them belong to one tridentate ligand and two chloride ligands. The APBH ligand is coordinated to central metal atom to form two five membered rings. One five-membered chelate ring consists of pyridine nitrogen and azomethine nitrogen and the other five membered chelate ring involves the azomethine and enolic oxgen donor atom. For five coordinate complexes, two polyhedra are considered: that is trigonal bipyramidal and square pyramidal. In our

Table 1 — Crystal data and structure refinement for the structure of Fe(APBH)Cl_2 complex

Structure parameter Data	
Empirical formula	$C_{14}H_{12}Cl_2FeN_3O$
Formula weight	365.02
Temperature	296(2) K
Wavelength	0.71073 Å
Crystal system	Monoclinic
Space group	$P2_1/n$
Unit cell dimensions	a = 7.8490(6) Å α= 90° b = 15.1018(11) Å β= 100.183(3)° c = 13.2263(10) Å γ= 90°
Volume	1543.1(2) $Å^3$
Z	4
Density (calculated)	1.571 Mg/m^3
Absorption coefficient	1.324 mm^{-1}
F(000)	740
Crystal size	0.150 x 0.100 x 0.100 mm^3
Theta range for data collection	2.065 to 24.888°
Index ranges	-7<=h<=9, -17<=k<=17, -15<=l<=15
Reflections collected	16392
Independent reflections	2691 [R(int) = 0.0409]
Completeness to theta = 24.888°	100.0 %
Absorption correction	Semi-empirical from equivalents
Max. and min. transmission	0.7451 and 0.6283
Refinement method	Full-matrix least-squares on F^2
Data / restraints / parameters	2691 / 0 / 191
Goodness-of-fit on F^2	1.106
Final R indices [I>2sigma(I)]	R1 = 0.0417, wR2 = 0.1006
R indices (all data)	R1 = 0.0834, wR2 = 0.1301
Extinction coefficient	n/a
Largest diff. peak and hole	0.345 and -0.486 e.$Å^{-3}$

Table 2 — Selected Bond lengths (Å) and Bond angles (°) for the structure of Fe(APBH)Cl_2

Bond Lengths		Bond Angles	
N(1)-Fe(1)	2.128(3)....	O(1)-Fe(1)-N(2).	74. 93(12)
N(2)-N(3)	1.382(4)...	O(1)-Fe(1)-N(1)	148.22(13)
N(2)-Fe(1)	2.074(3)...	N(2)-Fe(1)-N(1)	73.62(13)
O(1)-Fe(1)	1.954(3)...	O(1)-Fe(1)-Cl(2)	100.69(10)
Cl(1)-Fe(1)	2.2106(13). .	N(2)-Fe(1)-Cl(2)	130.32(10)
Cl(2)-Fe(1)	2.1914(13)	N(1)-Fe(1)-Cl(2)	96.09(10)
		O(1)-Fe(1)-Cl(1)	102.25(10)
		N(2)-Fe(1)-Cl(1)	118.35(10)
		N(1)-Fe(1)-Cl(1)	96.55(10)
		Cl(2)-Fe(1)-Cl(1)	110.99(6)

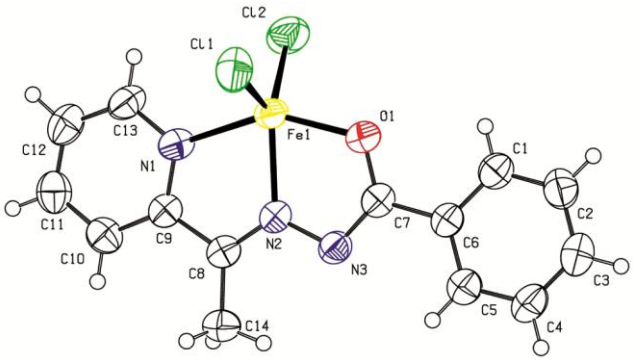

Fig. 2 — ORTEP plot for Fe(APBH)Cl_2 complex showing ellipsoids drawn at 50% probability.

case, the coordination polyhedron around iron atom is a distorted square pyramidal as shown in Fig. 2. The approximate square is formed with N_1, N_2, O_1 and Cl_2 atoms and Cl1 is present in axial position to complete distorted square pyramidal structure. The atoms of APBH ligand are almost located in the same plane. The Fe–N_1 and Fe–N_2 bond lengths are 2.128(3) and 2.074(3) Å, respectively. The Fe─N bond length data suggest that Fe–N(azomethine) is stronger than Fe–N(py) bond The Fe–O_1 bond length is 1.954(3) Å. The Fe–O bond distance is shorter than any Fe–N bond as expected for a hard oxygen atom bonded to transition metal ion. Similarly Fe–Cl_1 and Fe–Cl_2 bond lengths are 2.2106(13) and 2.1914(13) Å, respectively. Two different iron–chloride bond lengths suggest that they are present in two different planes viz. equatorial and axial positions.

Supra molecular interactions

Hydrogen bonding data for the structure of $Fe(APBH)Cl_2$ are given in Table 3. Among all contacts, H-bonds are the strongest and the most directional interactions that play the dominant role in the crystallization and stability of organic solids, π bond and stable H-bonding make the motif in supra molecular arrangement. In present, iron complexes, both intra and inter molecular hydrogen bonds of C1–H…O1, C12–H12···O1^{i} and C2–H2···Cl2^{i} forms the supramolecular network. The interactions of the hydrogen bonding are given in Table 3. Packing of molecules indicating Intermolecular (C–H…O and C–H…Cl) interactions and molecules with Cl- π and π–π interactions are shown in Figs. 4 and 5, respectively.

Anti bacterial activity studies

The antibacterial activities of 2-acetylpyridine acetoylhydrazone (APAH), 2-acetylpyridine benzoyl hydrazone (APBH), 2-acetylthiophene acetoylhydra zone (ATAH), and 2-acetylpyridine benzoylhydra zone (ATBH) and their iron complexes were investigated. The diameters (mm) of the zones of complete inhibition are given in Table 4. The antibacterial activities of our compounds are comparable to the activity of the standard drug, Streptomycin. APAH shows more activity than APBH. Similarly, ATAH is more active than ATBH. This trend indicates that acetoylhydrazones are more active than benzoylhydrazones against gram positive and gram negative bacteria. APAH is more active than ATAH and APBH is more active than ATBH. This trend suggest that the pyridine based hydrazones show more activity than thiophene based hydrazones against gram positive and gram negative bacteria.

A comparison (Table 4) of growth inhibition zones of ligands and their metal complexes indicates that metal complexes exhibit higher anti-bacterial activity than the free ligand, in analogy with previous

Table — 3 Hydrogen-bond geometry (Å, °) for $Fe(APBH)Cl_2$

D—H···*A*	*D*—H	H··· *A*	*D*···*A*	*D*—H···*A*
C1 – H1 … O1	0.93	2.48	2.786(5)	100
C12—H12···O1^{i}	0.93	2.65	3.503 (6)	152
C2—H2···Cl2^{i}	0.93	2.92	3.744 (3)	148

Symmetry code: (i) *x*-1/2, -*y*+3/2, *z*+1/2

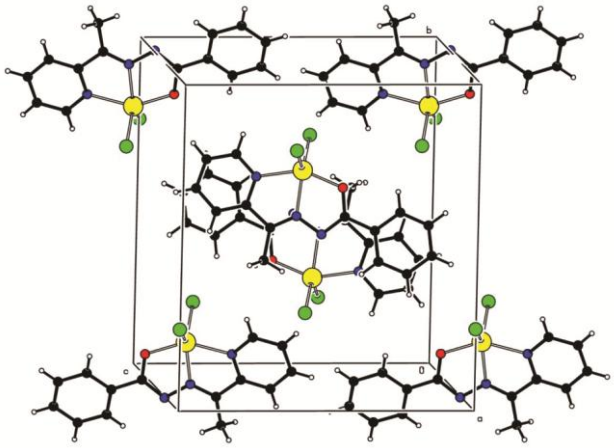

Fig. 3 — Packing of molecules in the unit cell of $Fe(APBH)Cl_2$ Complex.

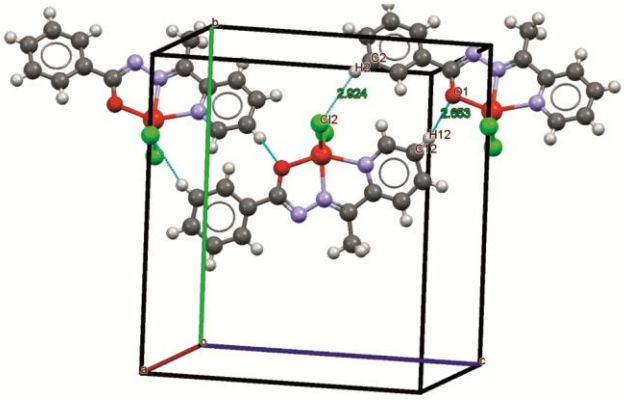

Fig. 4 — Packing of molecules indicating Intermolecular C–H…O and C–H…Cl interactions in $Fe(APBH)Cl_2$ Complex.

Table 4 — Zone of Inhibition (mm) data showing antibacterial activity of ligands and their iron complexes

Compound	Gram Positive *P.aureoginosa*			Gram Negative *Bacillus cereus*		
	200 µg/mL	300 µg/mL	500 µg/mL	200 µg/mL	300 µg/mL	500 µg/mL
APAH	7.0	8.0	8.5	5.0	6.0	6.5
$Fe(APAH)Cl_2$	8.2	9.0	9.5	7.2	8.3	8.0
APBH	6.0	7.0	7.5	5.0	5.5	6.0
$Fe(APBH)Cl_2$	8.5	7.5	8.0	6.5	7.2	8.5
ATAH	5.0	6.0	7.0	5.0	6.0	7.0
$Fe(ATAH)Cl_2$	6.0	6.7	7.5	5.5	6.5	7.0
ATBH	5.0	5.0	6.0	4.0	5.0	6.0
$Fe(ATBH)Cl_2$	5.5	6.0	7.0	5.5	6.0	6.5
Streptomycin	7.0	8.0	10.0	6.6	7.5	9.5

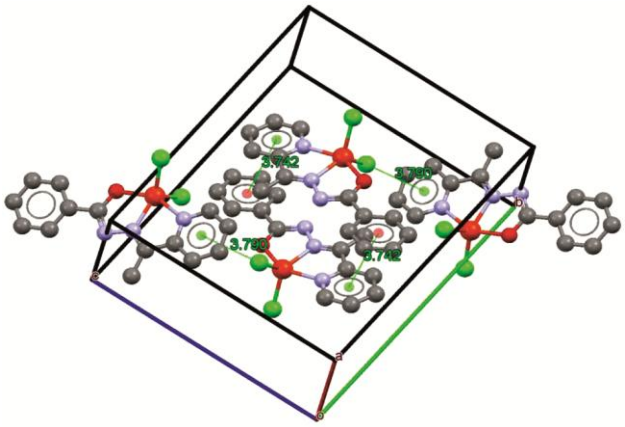

Fig. 5 — Packing of molecules with Cl … π and π – π stacking interactions in Fe(APBH)Cl_2 Complex.

observation[48-50]. Such increased activity of metal complexes is explained on the basis of *chelation*. The enhanced activity of the complexes can be explained on the basis of Overtone's concept[51] and *Tweedy's Chelation theory*[52]. According to the overtone concept of cell permeability, the lipid membrane surrounding the cell favours the passage of only lipid-soluble materials, which means that liposolubility is an important factor for controlling antimicrobial activity. On chelation, the polarity of a metal ion is greatly reduced due to overlap with the ligand orbital and the partial sharing of its positive charge with the donor groups. In addition, it is also due to delocalization of the π-electrons over the whole chelating ring, thus enhancing the penetration of the complexes into the lipid membranes and the blocking of the metal binding sites of the enzymes of the microorganisms[53].

Conclusions

Iron(III) complexes of hydrazone functionalized pyridine ligands were synthesized and characterized. The structure of Fe(APBH)Cl_2 complex is determined by using single crystal X-ray diffraction studies for the first time. Interestingly, here iron is five coordinated and the complex has a distorted square pyramidal structure. The complex has two labile ligands. Packing of molecules indicates intermolecular (C–H…O and C–H…Cl) interactions with Cl–Pi and Pi–Pi interactions. Antibacterial activity of ligands and their iron complexes are investigated in the present work. The data indicate that the pyridine based hydrazones show more activity than thiophene based hydrazones against gram positive and gram negative bacteria. Iron(III) complexes with hydrazones exhibit higher anti-bacterial activity than the iron free ligands.

Supplementary Data

Supplementary data associated with this article are available in the electronic form at http://www.niscair.res.in/jinfo/ijca/IJCA_59A(05)608-615_SpplData.pdf. CCDC No. 1869867 contains the supplementary crystallographic data for Fe(APBH)Cl_2 complex. These data can be obtained free of charge via http://www.ccdc.cam.ac.uk/conts/retrieving.html or from the Cambridge Crystallographic Data Centre,12 Union Road, Cambridge CB2 IEZ, UK; fax: +44 1223 336 033; or e-mail: deposit@ccdc.cam.ac.uk.

Acknowledgements

One of the authors (KHR) is thankful to University Grants Commission, New Delhi, India for the award of UGC-BSR Faculty Fellowship. The authors also thank UGC and DST for providing equipment facility under SAP and FIST programs, respectively. The authors also thank SAIF, IIT Madras for providing single crystal X-ray crystallographic data of iron complex.

References

1 Bertini I, Gray HB, Lippard, S J & Valentine J S, *Bioinorganic Chemistry*, Viva Low-Priced Edition, New Delhi (1998).
2 Hussain Reddy K, Cheng Z, Chada R, & Schrauzer G N, *Inorg Chem*, 30 (1991) 3865.
3 Tamasi G, Chiasserini L, Savini L, Sega A & Cini R J, *Inorg Biochem*, 99 (2005**)** 1347.
4 Sriram D, Yogeeswari P & Madhu K, *Bioorg Med Chem Lett*, 15 (2005) 4502.
5 El-Sherif A A, *Inorg Chim Acta*, 362 (2009) 4991.
6 Ahamed M J, Chowdhury D A, Uddin M N, Hossain K J, Choudhury M D A & Jannat T, *Pak J Anal Chem*, 5 (2004) 48.
7 Al-Hazmi G A & El-Asmy A A, *J Coord Chem*, 62 (2009) 337.
8 Zani V P, Cozzini F & Doytchinova P I, *Eur J Med Chem*, 37 (2002) 553.
9 Rollas S, *Farmaco* 57 (2002) 595.
10 Ragavendran J V, Sriram D, Patel S K, Reddy I V, Bharathwajan N, Stables J & Yogeeswari P, *Eur J Med Chem.* 42 (2007) 146.
11 Bezerra-Netto H J C, Lacerda D I, Miranda A L P, Alves H M, Barreiro E J & Fraga C A M. *Bioorg Med Chem*, 4 (2006) 7924.
12 Avaji P G, Kumar C H V, Patil S A, Shivananda K N & Nagaraju C, *Eur J Med Chem*, 44 (2009) 3552.
13 Kümmerle A E, Raimundo J M, Leal C M, Da Silva G. S, Balliano T L, Pereira M A, De Simone C A, Sudo R T, Zapata-Sudo G, Fraga C A M & Barreiro E J, *Eur J Med Chem*, 44 (2009) 4004.
14 Easmon J, Purstinger G, Roth T, Fiebig H, Jenny M, Jaeger W, Heinisch G & Hofmann J, *Int J Cancer*, 94 (2001) 89.
15 Richardson D R, Kalinowski D S, Richardson V, Sharpe P C, Lovejoy D B, Islam M & Bernhardt P V, *J Med Chem*, 52 (2009) 1459.

16 Stelzig L, Kotte S & Krebs B, *J Chem Soc Dalton Trans*, (1998) 2921.
17 Rana A, Dinda R, Sengupta P, Ghosh S & Falvello L R, *Polyhedron*, 21 (2002) 1023.
18 Rana A, Dinda R, Ghosh S & Blake A, *Polyhedron*, 22 (2003) 3075.
19 Tandon S S, Chander S & Thompson L K, *Inorg Chim Acta*, 300-302 (2000) 683.
20 Nazir H, Yildiz M, Yilmaz H, Tahir M N & Ulku D, *J Mol Struct*, 524 (2000) 241.
21 Nagawa N, Naseer M H, *Chem Pharm Bull*, 47 (1999) 944.
22 Easmon J, Purstinger G, Thies K S, Heinisch G & Hofmann J, *J Med Chem*, 49 (2006) 6343.
23 Paul V B, Gregory J W, Philip C S, Danuta S K & Des R R, *J Biol Inorg Chem*, 13 (2008) 107.
24 Angel A R D, Lorena F V, Isolda C M, Fernanada B C, Nivaldo L S & Heloisa B, *J Braz Chem Soc*, 21 (2010) 1247.
25 Angel A R D, Gabrieli I P, Jans B I, Pryscila R D, Raquel S, Oscar E P, Edurado E C, William R R & Helosia B, *Eur J Med Chem*, 50 (2012) 163.
26 Alangesan M, Bhuvanesh N S P & Dharmaraj N, *Dalton Trans*, 42 (2013) 7210.
27 Jeffery J C, Thornton P & Ward M D, *Inorg Chem*, 33 (1994) 3612.
28 Dutta S K, Tiekink E R T & Chaudhury M, *Polyhedron*, 16 (1997) 1863.
29 Scovill J P, *Phosphorus Sulfur and Silicon*, 60 (1991) 15.
30 Pessoa J C, Tomaz I & Henriques R T, *Inorg Chim Acta*, 356 (2003) 121.
31 Ando R, Yagyu T & Maeda M, *Inorg Chim Acta*, 357 (2004) 2237.
32 Ando R, Mori S, Hayashi M, Yagyu T & Maeda M, *Inorg Chim Acta*, 357 (2004) 1177.
33 Jang Y J, Lee U K, & Koo B K, *Bull Korean Chem Soc*, 26 (2005) 925.
34 Moksharagni B, Rishitha M & Hussain Reddy K, *Ind J Chem*, 56A (2017) 232.
35 Hari Babu P, Hussain Reddy K, Patil Y P & Nethaji M, *Ind J Chem*, 52A (2013) 327.
36 Pragathi M & Hussain Reddy K, *Ind J Chem*, 52A (2013) 845.
37 Hari Babu P, Hussain Reddy K, Patil Y P & Nethaji M, *Inorg Chim Acta*, 392 (2012) 478.
38 Pragathi M & Hussain Reddy K, *Inorg Chim Acta*, 413 (2014) 174.
39 Siemens, SMART SAINT, Area Detector Control and Integration Software, (Siemens Analytical X-ray Instruments Inc, Madison, Wisconsin, USA) (1996).
40 Sheldrick G M, *Acta Crystallogra A*, 46 (1990) 467.
41 Sheldrick GM, SHELXS-97, Program for the Solution of Crystal Structures, (University of Gottigen, Germany) (1997).
42 Brandenburg K & Purz H, DIAMOND version 3.0 *Crystal Impact*, GbR, Postfach 1251, D-53002 Bonn, Germany (2004).
43 Geary W J, *Coord Chem Rev*, 7 (1971) 81.
44 Ramasamy M, Sankaralingam M Suresh E & Palaniandavar M, *Daltons Trans*, 39 (2010) 9611.
45 Shebl M, *J Coord Chem*, 69 (2016) 199.
46 Kumar D N & Garg B S, *Spectrochim acta A*, 64 (2006) 141.
47 Raja K, Suseelamma A & Hussain Reddy K. *J Chem Sci*, 128 (2016) 23.
48 Prasad R V & Thakkar N V, *J Mol Catal*, 92 (1994) 9.
49 Belaid S, Landreau A, Djebbar S, Benali-Baitich O, Khan M A & Bouet G, *J Inorg Biochem*, 102 (2008) 63.
50 Dharmaraj N, Viswanathamurthi P & Natarajan K, *Trans Met Chem*, 26 (2001) 105.
51 Tweedy B G, *Phytopathology*, 55 (1964) 910.
52 Neelakanta M A, Esakkiammal M, Mariappan S S, Dharmaraja J & Jeyakumar T, *Ind J Pharm Sci*, 72 (2010) 216.
53 Chohan Z H, Misbahul A K, Moazzam M, *Ind J Chem*, 27A *(*1988) 1102.